



Utilization of activated carbon for the adsorption of methylene blue from waste coffee husk

Nguyen Thi Hong Phuong^{1,*}, Nguyen Thi Thu Huong², Nguyen Thu Ly³, Nguyen Thi Thu³,
 Nguyen Thi Thu Hang³, Hoang Thu Huong⁴, Nguyen Tien Dung⁴

¹ School of Chemistry and Life Sciences, Hanoi University of Science and Technology, 1 Dai Co Viet, Hanoi, Vietnam

² Academy of Military Science and Technology, 17 Hoang Sam, Hanoi, Vietnam

³ Joint Vietnam - Russia Tropical Science and Technology Research Center, 63 Nguyen Van Huyen, Hanoi, Vietnam

⁴ Faculty of Chemistry, Hanoi National University of Education, 136 Xuan Thuy, Hanoi, Vietnam

* Email: phuong.nguyenthihong@hust.edu.vn

ARTICLE INFO

Received: 01/12/2024

Accepted: 20/12/2024

Published: 30/03/2025

Keywords:

Activated carbon

Waste coffee husk

Adsorption

Methylene blue

ABSTRACT

This study investigated the pyrolysis of coffee husks to produce activated carbon (AC) and its effectiveness in adsorbing methylene blue (MB) from wastewater. Various techniques, including physical adsorption, Fourier transform infrared spectroscopy, X-ray diffraction, and scanning electron microscopy, were employed to analyze the sorbent. Several experiments were conducted to evaluate the effects of initial pH, adsorption duration, and MB concentration on the process. The results indicated that the optimal equilibrium time for AC adsorption was 60 minutes. The activated carbon exhibited a substantial surface area of 184.535 m²/g and was composed of heterogeneous, fibrous, and mineralized particles, primarily silica. The pH of the medium influenced the removal efficiency of MB. Kinetic data analysis showed that the second-order kinetic model described the adsorption process more accurately than other models, suggesting that MB diffusion occurred within the pores of the AC. However, this was not the only mechanism at play, as indicated by the applicability of the Elovich, Bangham, and intraparticle diffusion models. In terms of isotherm models, the Redlich-Peterson model provided the best fit when compared to the Freundlich, Temkin, and Sips models, reflecting the adsorption behavior at equilibrium. These findings highlight the significant potential of coffee husks as a low-cost alternative to commercial activated carbon for treating dye-laden wastewater.

Introduction

Annually, over 700,000 tons of 100,000 types of dyes are produced for various industries, with methylene blue (MB) being one of the most commonly used [1, 2]. Due to its aromatic structure, MB is highly toxic and difficult to treat, causing severe water pollution and

posing risks to ecosystems and human health [1]. As a result, MB removal from wastewater has become a significant focus, especially in Vietnam. While methods like ozonation, electrochemical treatments, and membrane separation exist, they are often costly and may produce more toxic by-products [2-4]. Adsorption is considered the most effective solution due to its high

removal efficiency, low cost, and simplicity [1, 5]. Activated carbon is widely used for this purpose. However, AC reuse is costly but has poor efficiency [1, 4]. Consequently, low-cost agricultural by-products, such as orange peel, coconut shell, and corn cob, are being explored for dye removal, demonstrating good performance [1, 2].

Conventional activated carbon production involves two steps: carbonization and activation [5]. Carbonization involves heating biomass at high temperatures (350–900 °C) in an inert or oxygen-free environment to obtain biochar. Activation involves heating acid/alkali-impregnated biochar [6]. These two steps are energy-intensive, require large amounts of biomass input, and consume non-recyclable reactants [1, 7]. To address these drawbacks, a simpler, cost-effective method using coffee husks as a by-product source has been proposed. Coffee husks, which account for about 12 % of the weight of dry-processed coffee beans, are therefore readily available in Vietnam, as Vietnam is the second largest exporter of coffee beans in the world [8]. With their composition of cellulose, hemicellulose, lignin, and ash [4], coffee husks can be repurposed as effective, low-cost bioadsorbents.

This study aimed to evaluate the adsorption capacity of activated carbon (AC) derived from coffee husks under various experimental conditions. The experiments were conducted to determine optimal factors including initial pH, initial dye concentration, and contact time. By employing kinetic modeling studies, adsorption isotherms, and examining the equilibrium and mechanisms of methylene blue (MB) adsorption by biochar, the study provided a detailed analysis of the adsorption capacity and the interaction mechanisms involved.

Experimental

Materials

Methylene blue (MB), used in the experiments, was of analytical grade and obtained from Xilong (China). Sodium hydroxide (NaOH) and hydrochloric acid (HCl), also of analytical grade, were sourced from Merck. Distilled water was employed for preparing solutions and for cleaning glassware.

Synthesis of activated carbon

The AC used in this study was sourced from coffee husks collected in Dak Lak, Vietnam. The activated

carbon from coffee husks was prepared in two steps. In the first step, the coffee husks were pyrolyzed at 450 °C for 30 min to produce biochar. In the second step, this biochar was physically activated at 900 °C for 1 h. Both steps were conducted under controlled conditions, with an airflow rate of 100 cm³/min and a heating rate of 10 °C/min in a nitrogen atmosphere. Prior to analysis, the activated carbon was sieved to a pore size of 250 μm.

Characterization of activated carbon

The morphology of the AC was analyzed using a high-resolution scanning electron microscope (JSM-IT800) with an X-ray spectroscopy detector. X-ray diffraction was used to determine the crystal structure of the AC sample before and after methylene blue adsorption with 2θ range from 10° to 70°. Specific surface areas were calculated using nitrogen adsorption/desorption isotherms and the BET method. Surface functional groups were identified using FTIR spectroscopy in the 4000–400 cm⁻¹ range.

Methylene Blue adsorption on activated carbon

Batch adsorption experiments were conducted to evaluate the effects of time, initial solution pH, and initial concentration on the removal of methylene blue (MB). Each experiment involved shaking 50 mL of MB solution with 0.05 g of activated carbon (AC) in a 100 mL flask at a speed of 150 rpm. The pH effect was analyzed within a range of 3 to 11, adjusted using 0.1 M hydrochloric acid (HCl) or 0.1 M sodium hydroxide (NaOH), and the mixtures were shaken for 60 minutes at a temperature of 298 K. The initial MB concentrations varied from 10 to 50 mg/L, with contact times ranging from 15 to 75 minutes at the same temperature. After shaking, the supernatant was filtered and analyzed using UV-Vis spectroscopy. The concentration of MB in the solutions was quantified with a UV-Vis spectrophotometer (DV-8200 from Drawell, China) at a wavelength of 662 nm. The adsorption capacity and the percentage of MB removal were calculated using specific equations.

$$q = \frac{(C_0 - C_t) \times V}{m} \quad (1)$$

$$H = \frac{(C_0 - C_t) \times 100}{C_0} \quad (2)$$

Where q (mg g⁻¹) is the MB adsorption capacity of AC, C_0 (mg L⁻¹) is the initial concentration of MB, C_t (mg L⁻¹) is the MB concentration at time t (min), V (mL) is the solution volume, and m (mg) is the AC mass. H (%) is the removal efficiency.

Adsorption kinetics and equilibrium

Adsorption kinetics and equilibrium experiments were conducted at 25°C (298 K) with a natural pH using 50 mL of methylene blue (MB) solution at initial concentrations ranging from 10 to 50 mg/L, along with 50 mg of dry activated carbon (AC). The experimental data were analyzed using various adsorption kinetics and equilibrium models (refer to Table S1 and Table S2, Supporting information). Pseudo-first-order models are appropriate for describing physical adsorption processes, whereas pseudo-second-order models are more suitable for chemical adsorption processes. The pseudo-second-order model assumes that adsorption is proportional to the number of active sites. The rate of MB adsorption (h) for the material was calculated using Equation (3).

$$h = k_2 q_e^2 \quad (3)$$

In which, q_e (mg g^{-1}) is the amount of adsorbent at equilibrium; k_2 ($\text{g mg}^{-1} \text{min}^{-1}$) is the constant rate of Pseudo-second order;

The Elovich model considers that the active sites of the adsorbent are heterogeneous, resulting in different activation energies. The Bangham model is applied to assess whether pore diffusion is the only rate-controlling step in the adsorption process. Meanwhile, the Intraparticle Diffusion model posits that the rate of adsorption is exclusively governed by intra-particle diffusion, disregarding any external transport and membrane diffusion factors.

The reusability of activated carbon (AC) in methylene blue (MB) adsorption was assessed after the desorption of MB from AC using anhydrous ethanol before starting the next adsorption cycle.

Results and discussion

Characterization of activated carbon

Figure 1 (a, b) illustrates the surface morphology of coffee husk and activated carbon (AC). In this experiment, the coffee husks were pyrolyzed in an N_2 atmosphere without undergoing an activation step. As a result, the surface structure of the obtained activated carbon was more porous than that of the coffee husks, but not as porous as that of activated coffee husks [14]. This difference in porosity is believed to be influenced by the volatile organic compounds released during pyrolysis, which affect the porous structure of the AC.

AC has an uneven porous inner surface, ideal for adsorbing large organic molecules like MB. The EDX spectrum (Figure 1c) reveals that AC is mainly

composed of carbon, potassium, and calcium (CaCO_3 , feldspar, wollastonite) [4]. Nitrogen adsorption isotherms (Figure 1d) confirmed with a surface area of $184.535 \text{ m}^2/\text{g}$, pore volume of $0.07 \text{ cm}^3/\text{g}$, and pore radius of 1.68 nm.

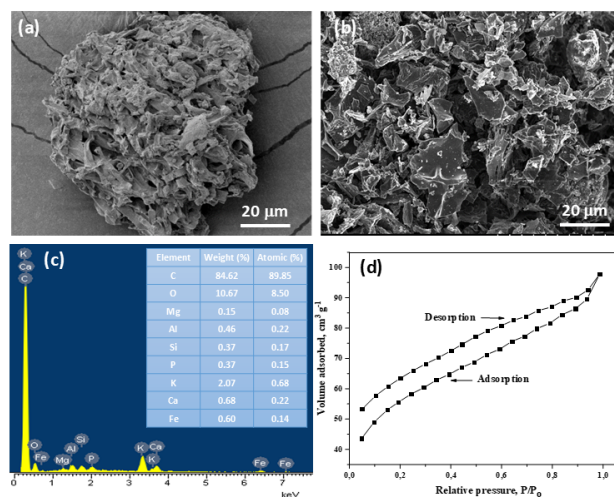


Figure 1: FE-SEM of coffee husk (a) and SEM of AC before adsorption (b) (magnification 1000 \times); EDX of AC before adsorption (c); Nitrogen adsorption/desorption isotherm at 77K (d)

FTIR spectra of AC before and after MB adsorption (Fig. 2a), showing the changes in functional groups and surface properties of AC. The characteristic peaks observed in the range of $3255\text{--}3504 \text{ cm}^{-1}$ indicate the presence of free hydroxyl groups from carboxylic acids, phenols, alcohols, and other organic substances that contain hydroxyl ions found in cellulose and lignin. It is noted that the transmittance value of activated carbon (AC) before adsorption is higher than that after adsorption. This change is attributed to the fact that the active sites on the AC become occupied by methylene blue (MB) molecules after adsorption. The results confirm that the surface of the AC is occupied by MB, leading to a decrease in transmittance following adsorption. Additionally, the peak at 1032 cm^{-1} in the AC before adsorption corresponds to the C–O–C stretching vibrations found in esters, ethers, or phenols. After MB adsorption, the peak at 1573 cm^{-1} in the AC sample indicates an increase in $\text{C}=\text{C}$ bonds, likely resulting from the adsorption of MB onto the AC. The reduction of the carboxylic group ($\text{C}=\text{O}$), peak at 1618.77 cm^{-1} is believed to be related to the carboxylate group [1]. The peak at 1486.11 cm^{-1} and 1431 cm^{-1} may be $\text{C}=\text{C}$ bond in the aromatic ring, which may be the result of electrostatic attraction between the negative charge of carboxylic group ($\text{C}=\text{O}$) ions and the positive charge in MB [4]. The change in peak at 1391.18 cm^{-1}

reflects the stretching vibration of the carboxylic group (-COOH) [5]. The peak at 1067.07 cm^{-1} is believed to be the stretching of C-O containing functional groups [4]. This indicates that AC has the potential to be used as a dye adsorbent [11].

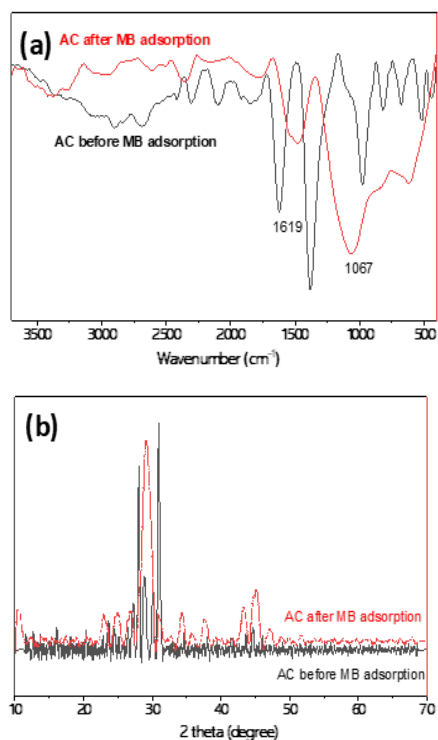


Figure 2: FTIR (a) and XRD (b) of AC before and after MB staining

XRD analysis was conducted to investigate the crystalline nature of the adsorbent, as shown in Figure 4a. The peak within the range of 2θ from 10° to 40° is associated with the amorphous phase, characteristic of lignocellulosic biomass [1]. The presence of ridges in the diffraction pattern indicates a high degree of disorder, which is a typical feature of carbonaceous materials [2]. Similar XRD spectra were observed for activated carbon (AC) prepared from various biomass sources [3]. Peaks at $2\theta = 23^\circ$ to 25° were assigned to planar graphite (002), suggesting the presence of several stacked carbon layers alongside an amorphous structure [5]. The weak peak at 43.4° corresponds to the lattice plane (100), indicating an ordered hexagonal carbon structure known as graphitic carbon [6]. The presence of both peaks implies the formation of disordered carbonaceous materials with turbostratic structures or random layered lattice structures [3]. After methylene blue (MB) adsorption, the XRD patterns of AC displayed peaks that shifted slightly to the left compared to the patterns before MB adsorption. However, these peaks were more pronounced and

broader at $2\theta = 23.0^\circ$, 25.0° , and 29.0° , while they were weaker at 30.9° , indicating the formation of carbon materials with a disordered structure [1]. Additionally, the peak at $2\theta = 28^\circ$ disappeared, which is believed to be due to the absence of the adsorption peak related to biomass-derived carbon [7]. Furthermore, the peak intensities changed, and some new weak peaks appeared in the XRD patterns of activated carbon after adsorption, as illustrated in Figure 4a. These changes are thought to be a result of MB adsorption [5]. The broadening of the peak intensities suggests an improved layer arrangement and a consistent increase in the crystal structure [8].

Methylene Blue adsorption on activated carbon

The removal efficiency of methylene blue (MB) was found to be directly proportional to the concentration of the adsorbent, as shown in Figure 3. This relationship may be attributed to the increased availability of adsorption sites resulting from a higher adsorbent concentration, which in turn enhances the surface area of activated carbon (AC). For this study, an MB concentration of 10 mg L^{-1} was selected to evaluate the adsorption capability of AC.

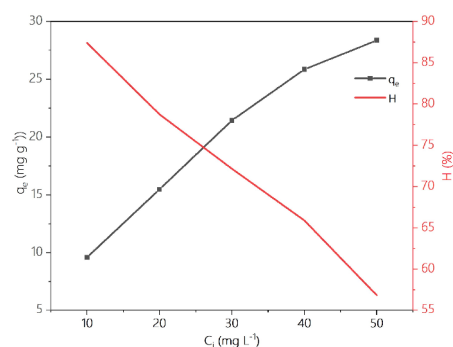


Figure 3: MB adsorption capacity of AC ($C_0 = 10\text{ mg L}^{-1}$, $m = 0.05\text{ g}$, $t = 24\text{ h}$, $V = 50\text{ mL}$, $T = 298\text{ K}$).

Figure S1a (shown in Supporting information) presents the pH at the point of zero charge (pH_{zpc}) results for the tested sample. The pH_{zpc} of the adsorbent was found to be 9.25. Since methylene blue (MB) is a cationic dye and activated carbon (AC) gradually converts to a cationic form while releasing anions, the adsorption of MB becomes favorable at a pH higher than 9.25. At acidic pH, AC had the maximum adsorption capacity for eliminating MB from aqueous solution, and at alkaline pH, this capacity progressively declined. However, the adsorption capacity achieved saturation at pH values greater than 7 (Figure S1b). This is explained by the modification of the MB ionization state and the surface area of AC in solution at various pH values [1, 12]. As a result, the initial pH has a

significant influence on the adsorption capability of AC for MB, with neutral and acidic pHs being preferred. Similar findings were reported by [4, 5].

The contact time required for the adsorption of MB onto activated carbon (AC) to reach equilibrium is illustrated in Figure S1c (shown in Supporting information). The rapid decrease in MB concentration within the first 60 minutes may be attributed to the abundance of free sites on the AC surface. As MB molecules gradually penetrate the internal sites of the AC through membrane and pore diffusion, the repulsion between them increases once the available adsorption sites become saturated. This leads to the equilibrium point being achieved at 60 minutes, indicating the maximum adsorption capacity. Moreover, the removal of MB from coffee husks via pyrolysis is more cost-effective and efficient compared to other commercial solids, which have an equilibrium period of approximately 720 minutes [13]. This increased efficiency is due to the effectiveness of mechanisms such as hydrogen bonding, pi stacking, electrostatic attraction, and Van der Waals forces in facilitating MB removal [14].

Adsorption kinetics

Table 1 and Figure 4 present the kinetic model parameters. Although the first-order model has the highest R^2 , the experimental adsorption capacity ($q_{e,exp}$) aligns better with the calculated value from the second-order model ($q_{e,cal}$), making the second-order model more suitable for describing MB adsorption onto AC. This suggests that the process is controlled by a chemical reaction mechanism [1]. The h value indicates surface exchange reactions until the energy sites are occupied. The Elovich and Bangham models show poor fits with low R^2 values. The Intraparticle diffusion model (Figure 5) reveals that while intra-particle diffusion contributes, other mechanisms also play a role.

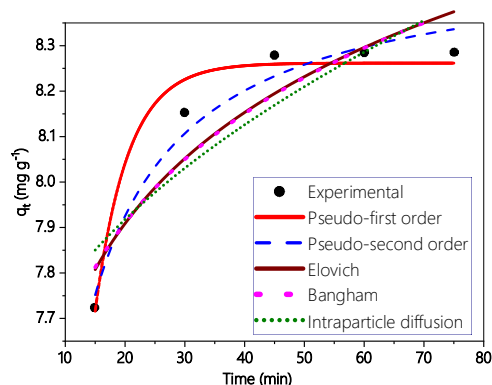


Figure 4: First-order, second-order, Elovich, Bangham and Intraparticle diffusion kinetic models fit the experimental data ($C_0=10 \text{ mg L}^{-1}$, $m=0.05 \text{ g}$, $V=50 \text{ mL}$, $T=298\text{K}$)

Table 1: Characteristic parameters, R^2 and χ^2 for first-order, second-order, Elovich, Bangham and Intraparticle diffusion kinetic models.

Models	Parameters	Value
		$q_{e,exp} \text{ (mg g}^{-1}\text{)}$
<i>Pseudo-first order</i>	$q_{e,cal} \text{ (mg g}^{-1}\text{)}$	8.26173
	$k_1 \text{ (min}^{-1}\text{)}$	0.18114
	R^2	0.97069
	χ^2	0.00227
<i>Pseudo-second order</i>	$q_{e,cal} \text{ (mg g}^{-1}\text{)}$	8.49645
	$k_2 \text{ (g mg}^{-1} \text{ min}^{-1}\text{)}$	0.08165
	$h \text{ (mg g}^{-1} \text{ min}^{-1}\text{)}$	5.89427
	R^2	0.96704
	χ^2	0.00256
<i>Elovich</i>	$\beta \text{ (g mg}^{-1}\text{)}$	2.8377
	$\alpha \text{ (mg g}^{-1} \text{ min}^{-1}\text{)}$	9.83714E7
	R^2	0.86191
	χ^2	0.01071
<i>Bangham</i>	$k_B \text{ (mg g}^{-1} \text{ s}^{-\alpha}\text{)}$	6.94957
	α	0.04322
	R^2	0.8548
	χ^2	0.01127
<i>Intraparticle diffusion</i>	$K_{i1} \text{ (mg g}^{-1} \text{ min}^{-0.5}\text{)}$	0.11242
	C_1	7.41498
	R_1^2	0.7715

Adsorption isotherm

Figure 5 and Table 2 indicate that the Redlich-Peterson model provides the best fit for the adsorption of methylene blue (MB) onto activated carbon (AC), as evidenced by the highest R^2 and lowest χ^2 values.

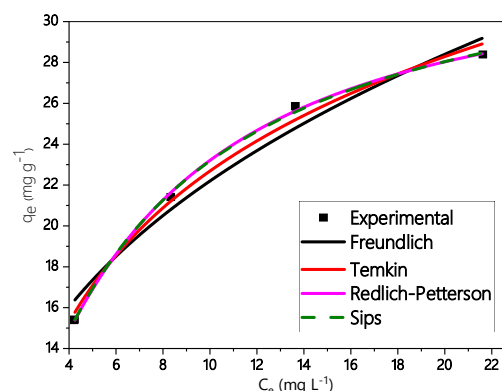


Figure 5: Freundlich, Temkin, Redlich-Peterson, and Sips adsorption isotherms ($m=0.05 \text{ g}$, $V=50 \text{ mL}$, $T=298\text{K}$).

Table 2: Characteristic parameters, R^2 and χ^2 for Freundlich, Temkin, Redlich-Petterson, and Sips adsorption isotherms.

Models	Parameters	Value
<i>Freundlich</i>	$K_F [(mg\ g^{-1})(L\ mg^{-1})^{1/n}]$	9.79022
	$1/n$	0.35551
	R^2	0,95326
	χ^2	1,49133
<i>Temkin</i>	b_T	8.08205
	A	1.65602
	R^2	0,98669
	χ^2	0.4247
<i>Redlich-Petterson (RP)</i>	$K_{RP} (L\ g^{-1})$	5.80702
	$\alpha (L\ mg^{-1})^\beta$	0.12934
	β	1.0
	R^2	0.99662
<i>Sips</i>	χ^2	0.1077
	$Q_{max} (mg\ g^{-1})$	34.43641
	$K_S (L\ mg^{-1})$	0.19394
	$1/n$	1.0
	R^2	0.99595
	χ^2	0.12927

Additionally, other models, including Freundlich, Temkin, and Sips, were also evaluated to describe the adsorption equilibrium of AC on MB (Figure S2, Supporting information). The Freundlich model highlights the heterogeneity of energy on the surface of AC, characterized by the parameter n . A value of $1/n$ (0.35551) suggests that approximately 36% of the adsorption sites have uniform energy, while the remaining 64% exhibit varying energy levels (Table 4). The K_F value reflects the capacity of the adsorption process. Both the Redlich-Peterson and Sips models depict a hybrid isotherm that combines aspects of the Langmuir and Freundlich models. The findings imply that the adsorption of MB is influenced by chemical interactions with surface functional groups and binding energy [1, 15]. Therefore, coffee husks emerge as a promising, low-cost, and effective adsorbent for the removal of MB from wastewater.

The ability to reuse saturated adsorbents is crucial for practical applications, as regenerating the adsorbent is necessary to sustain the process. Additionally, regenerating the adsorbent is more cost-effective than replacing it, thereby reducing the need for direct disposal of used adsorbents. To investigate this, we

examined the removal efficiency of methylene blue (MB) from the solution by activated carbon (AC) after five reuse cycles. The results presented in Figure 7 indicate that activated carbon (AC) can be used multiple times without significant loss of efficiency. After five reuse cycles, the removal efficiency of methylene blue (MB) from water decreased by less than 10%. Additionally, methylene blue can be effectively recovered from activated carbon after adsorption by using ethanol as a solvent.

Conclusion

This study demonstrated that activated carbon (AC) produced from coffee husks through pyrolysis is highly effective at removing methylene blue (MB) from wastewater. The material possesses a substantial surface area of $184.535\ m^2/g$ and has a heterogeneous structure primarily composed of carbon, calcium, and potassium. The experimental results were well-described by the Redlich-Peterson isotherm model, with a correlation coefficient (R^2) of 0.99662. Additionally, the quadratic model provided a detailed explanation of the adsorption kinetics. The pH of the environment significantly influences the elimination of MB, especially in acidic conditions. This research highlights the potential of agricultural by-products, such as coffee husks, in producing bio-activated carbon, which could serve as a substitute for commercial activated carbon in the adsorption of dyes and other pollutants in wastewater.

Acknowledgements

This work is conducted and funded by the School of Chemistry and Life Sciences, Hanoi University of Science and Technology. This work was also supported in part by the Department of Chemistry and Environment, Joint Vietnam-Russia Tropical Science and Technology Research Center.

References

1. T.H. Tran, A.H. Le, T.H. Pham, D.T. Nguyen, S.W. Chang, W.J. Chung, and D.D. Nguyen, *Sci. Total Environ.* 725 (2020) 138325. <https://doi.org/10.1016/j.scitotenv.2020.138325>
2. P. Deivasigamani, P.S. Kumar, S. Sundaraman, M.R. Soosai, A.A. Renita, M. Karthikeyan, N. Bektenov, O. Baigenzhenov, D. Venkatesan, and A. Kumar, *Environ. Res.* 236 (2023) 116735. <https://doi.org/10.1016/j.envres.2023.116735>

3. N.E.T. Castillo, J.S.O. Sierra, M.A. Oyervides-Muñoz, J.E. Sosa-Hernández, H.M. Iqbal, R. Parra-Saldívar, and E.M. Melchor-Martínez, *Case Stud. Chem. Environ. Eng.* 3 (2021) 100070. <https://doi.org/10.1016/j.cscee.2020.100070>
4. C.A. Andrade, L.A. Zambrano-Intriago, N.S. Oliveira, J.S. Vieira, L.S. Quiroz-Fernández, and J.M. Rodríguez-Díaz, *Water Air Soil Pollut.* 231 (2020) 1-16. <https://doi.org/10.1007/s11270-020-04473-6>
5. J.N. Njeri, E.W. Nthiga, and G.K. Muthakia, (2023). <https://doi.org/10.26438/ijsrcs/v10i4.19>
6. T. Van Limbergen, I.H. Roegiers, R. Bonn  , F. Mare, T. Haeldermans, B. Joos, O. Nouwen, J.V. Manca, J. Vangronsveld, and S. Thijs, *Front. Environ. Sci.* 10 (2022) 814267. <https://doi.org/10.3389/fenvs.2022.814267>
7. N.V. Phuong, N.K. Hoang, L.V. Luan, and L. Tan, *Int. J. Agron.* 2021 (2021) 1463814. <https://doi.org/10.1155/2021/1463814>
8. M. Konneh, S.M. Wandera, S.I. Murunga, and J.M. Raude, *Heliyon.* 7 (2021). <http://doi.org/10.1016/j.heliyon.2021.e08458>
9. J. Kochito, A. Gure, N. Abdissa, T.T. Beyene, and O.E. Femi, *Sci. World J.* 2024 (2024) 7585145. <https://doi.org/10.1155/2024/7585145>
10. T.K. Murthy, B. Gowrishankar, M.C. Prabha, M. Kruthi, and R.H. Krishna, *Microchem. J.* 146 (2019) 192-201. <https://doi.org/10.1016/j.microc.2018.12.067>
11. D.F.C. de Benedicto, G.M.D. Ferreira, and S.S. Thomasi, *Colloids Surf. A: Physicochem. Eng. Asp.* 701 (2024) 134921. <https://doi.org/10.1016/j.colsurfa.2024.134921>
12. V. Thi Quyen, T.-H. Pham, J. Kim, D.M. Thanh, P.Q. Thang, Q. Van Le, S.H. Jung, and T. Kim, *Chemosphere.* 284 (2021) 131312. <https://doi.org/10.1016/j.chemosphere.2021.131312>
13. M.Z.M. Mendonça, F.M. de Oliveira, J.M. Petroni, B.G. Lucca, R.A.B. da Silva, V.L. Cardoso, and E.I.J.J.o.A.E. de Melo, *J. Appl. Electrochem.* 53 (2023) 1461-1471. <https://doi.org/10.1007/s10800-023-01853-8>
14. N.-T. Vu, T.-H. Ngo, T.-T. Nguyen, and K.-U. Do, *Biomass Conv. Bioref.* (2021) 1-10. <https://doi.org/10.1007/s13399-021-01788-0>
15. A.E. de Castro, F. da Silva Martinho, M.L. Barbosa, J.R. Franca, J. Ribeiro-Soares, G.M.D. Ferreira, and G.M.D. Ferreira, *Water, Air, Soil Pollut.* 233 (2022) 180. <https://doi.org/10.1007/s11270-022-05623-8>